AMERICAN JOURNAL OF PHYSIOLOGY
CELL PHYSIOLOGY

*Am J Physiol Cell Physiol* 329: C585–C591, 2025.
*First published July 11, 2025; doi:10.1152/ajpcell.00424.2025*

SHORT REPORT

# Functional reassessment of Nav1.5 T559A reveals loss-of-function in a variant commonly used as wild type

**Dario Melgari,[1] Marco Villa,[1] Anthony Frosio,[1] Serena Calamaio,[2] Luigi Anastasia,[1,3] Carlo Pappone,[1,3] and Ilaria Rivolta[1,2]**

[1]*Institute of Molecular and Translational Cardiology, IRCCS Policlinico San Donato, Milan, Italy;* [2]*School of Medicine and Surgery, University of Milano-Bicocca, Monza, Italy; and* [3]*Faculty of Medicine and Surgery, Vita-Salute San Raffaele University, Milan, Italy*

## Abstract

*SCN5A* encodes the α-subunit of the cardiac voltage-gated sodium channel Nav1.5 that plays a fundamental role in the excitability and functionality of the human heart. Nav1.5 T559A is a rare variant that has never been functionally characterized nor clinically described. However, it is present in the hH1a *SCN5A* clone that has been used as a wild-type control over the years. In this work, we performed a functional electrophysiological characterization of T559A by comparing it with the reverted channel T559. When expressed in a heterologous system, T559A resulted in a significant reduction in sodium current density, suggesting a loss-of-function effect of the mutation. Also, mutation reversion slightly but significantly accelerated the kinetics of both channel activation and inactivation. Thus, caution should be exercised in choosing the most appropriate control and genetic background in functional studies.

**NEW & NOTEWORTHY** This work represents the first functional characterization of the Nav1.5 T559A channel variant that has been widely used as a control wild type over the past decades. We found that the substitution T559A caused a loss-of-function reduction of current density, with smaller effects on channel kinetics and voltage-dependence.

*cardiac physiology; electrophysiology; patch-clamp; rare variant; sodium channel*

## INTRODUCTION

*SCN5A* encodes the α-subunit of the cardiac voltage-gated sodium channel Nav1.5 that plays a fundamental role in the excitability and functionality of the human heart. Its primary structure and functional expression were first described by Gellens et al. (1) in 1992 when the channel was cloned from a human cardiac cDNA library using probes derived from the rat muscle tetrodotoxin (TTX)-insensitive isoform (rSkM2). They named the newly sequenced protein "hH1" (GenBank ID: M77235) (1). A second variant was then cloned in 1994 by Hartmann et al. (2) as a chimeric cDNA construct between fetal RNA (≈75% of the full-length construct) and RNA obtained from frozen biopsy tissue of diseased adult ventricular myocardium. The Hartmann clone was one amino acid shorter than the original hH1 described by Gellens (missing a glutamine in position 1077, Q1077del) and was named "hH1a" (GenBank ID: NM_000335.5) (2). Later studies confirmed that the two clones represented splice variants of the cardiac sodium channel, with Q1077del being the preferred alternatively spliced variant among the two (3). However, hH1a also carried a substitution of a threonine with an alanine in position 559 compared with hH1 (T559A). This represents a rare variant with 0% frequency on the Genome Aggregation Database (GnomAD) and is absent from population consensus sequences. In fact, 100% of 400 reference alleles derived from the 100 Caucasian human variation panel (Coriell Cell Repositories) and the 100 African-American human variation panel (National Institute of General Medical Sciences) had a threonine in position 559. Moreover, T559 is also predicted by the deduced amino acid sequence for *SCN5A* obtained by both the International Human Genome Sequencing Collaboration (IHGSC) and the Celera human genome databases (3). Intriguingly, this variant slipped through the cracks, and several studies unknowingly used hH1a T559A as a wild-type (WT) control through the years (e.g., see Refs. 4–12). Since it was never associated with any clinical case report, T559A was never functionally characterized. Here, we studied the electrophysiological effects of this variant by reverting the mutation of hH1a to the expected threonine.

## MATERIALS AND METHODS

### Sequencing and Mutagenesis

hH1a *SCN5A* cDNA was subcloned into the pcDNA3.1 plasmid, with the enhanced green fluorescence protein (eGFP) linked to the *N*-terminal of the channel. The presence of the T559A variant and the lack of other polymorphisms were

Correspondence: I. Rivolta (ilaria.rivolta@unimib.it).
Submitted 28 May 2025 / Revised 10 June 2025 / Accepted 9 July 2025

assessed through full-length plasmid sequencing performed with Oxford Nanopore Technologies by the Microsynth AG company. The mutation was then reverted via site-directed mutagenesis with the QuikChange II site-directed mutagenesis kit (Agilent Technologies Italia), according to the manufacturer's instructions. The primers for reversion (c.1675 rev. G>A) were as follows:

AGAGCGAGAGCCACCAC**A**CATCACTGCTGGTGCCCT (Forward) and AGGGCACCAGCAGTGATG**T**GTGGTGG-CTCTCGCTCT (Reverse).

### Electrophysiology

HEK293T cell line was maintained and transiently transfected as previously described (13). The channel carrying the threonine in position 559 is named "reverted" (abbreviated to "REV") from now on in the manuscript. Manual patch-clamp experiments were conducted 72 h after the transfection with a 700B amplifier (Molecular Devices) in whole cell configuration. The external recording solution contained (in mM): NaCl 40, KCl 4, $CaCl_2$ 2, $MgCl_2$ 1, HEPES 10, *N*-methyl-D-glucamine (NMDG) 100, glucose 5 (pH 7.4 with NaOH, 305 mosmol/kg$H_2O$). To measure the small late sodium current, recordings were performed using a solution containing 140 mM NaCl (without NMDG). Tetrodotoxin (TTX, 30 μM) was applied to block $Na^+$ channel currents and isolate background activity. The late sodium current was defined as the TTX-sensitive component, calculated by subtracting the current recorded in the presence of TTX from that recorded in its absence. This difference was measured at the end of the depolarizing step (200 ms) and normalized to the peak current. The intracellular solution contained (in mM): CsF 110, CsCl 10, NaCl 10, HEPES 10, EGTA 10 (pH 7.2 with CsOH, >280 mosmol/kg$H_2O$). Glass pipettes were pulled with a horizontal P-1000 puller (Sutter Instruments) to a final resistance of 2–5 MΩ. Membrane capacitance and 80% series resistance were electronically compensated. Currents were sampled at 50 kHz and low-pass filtered at 10 kHz. Voltage protocols for current-voltage relationship, voltage-dependence of inactivation, and recovery from inactivation were performed as previously described (13). *I-V* recordings were online P/4 leak corrected during acquisition. All experiments were performed at room temperature.

### Analysis

Offline analysis was performed with Clampfit (Molecular Devices), Origin (OriginLab), and Prism (GraphPad) software. Data are represented as means ± SE ($n$ = number of cells; $N$ = number of experimental replicates).

Curves of voltage dependence of channel activation were built by plotting the normalized channel conductance ($G/G_{max}$) against the test voltage. Channel conductance for each cell was calculated with the equation:

$$G_x = \frac{I_x}{(V_x - E_{rev})}$$

where $I_x$ is the peak current amplitude at test voltage $V_x$ and $(V_x - E_{rev})$ is the calculated driving force.

Voltage dependence of channel activation and inactivation curves were fitted with the following standard Boltzmann sigmoidal equation:

$$y = \text{Bottom} + \frac{(\text{Top} - \text{Bottom})}{1 + e^{\left(\frac{V_{1/2} - x}{\text{Slope}}\right)}}$$

where $y$ is the normalized maximal conductance or maximal current, $x$ is the test voltage, Bottom and Top are the minimum and maximum values of the curves, respectively, $V_{1/2}$ is the half voltage of maximal activation or inactivation, and Slope is the slope factor of the curve.

Activation kinetics were calculated by fitting the activating peak current rising phase with the following standard single-exponential function:

$$y = \sum_{i=1}^{n} A_i e^{-x/\tau_i} + C$$

where $y$ is the current amplitude at time $x$, τ is the time constant, $A$ is the total fitted current, and $C$ is any unfitted residual current.

Inactivation kinetics were calculated by fitting the inactivating peak current decay with the double-exponential function of the form:

$$y = \sum_{i=1}^{n} A_{is} e^{-x/\tau_s} + A_{if} e^{-x/\tau_f} + C$$

where the variables and constants are similar to those of the single-exponential function, but the time constant is split into a slow (s) and a fast (f) component.

Statistical analysis was performed with the appropriate test required by the different data set.

## RESULTS

### T559A Reduces Current Density Compared with the Reverted Channel

The threonine in position 559 is located in the DI-DII intracellular loop (Fig. 1*A*) and is conserved within the primate order with the exception of the Orangutan (*Pongo pygmaeus abelii*) that carries an isoleucine. Moreover, the threonine in position 559 is widely conserved within the Mammalia class with the intriguing exception of the tenrec (*Echinops telfairi*), the Tasmanian devil (*Sarcophilus harrisii*), and the opossum (*Monodelphis domestica*) all carrying an alanine. Interestingly, outside the Mammalia class, birds, amphibians, reptiles, and fishes all carry a glycine in position 559 (Fig. 1*B*). Thus, the substitution with an alanine replaced a highly conserved polar hydrophilic residue with a nonpolar hydrophobic one within a highly phosphorylation-regulated region (14). The sodium currents conducted by Nav1.5 T559A (T559A) and the reverted channel (REV) were elicited from a holding potential of −120 mV with a series of 50 ms pulses between −80 and +60 mV with 5 mV increment (Fig. 2*A*). The reversion of the mutation almost doubled the peak-current density compared with T559A and significantly increased the maximal conductance (Fig. 2*B*, Table 1). Also, from the *I-V* curves, the reversal potential for both channels appeared to be ≈10 mV rightward shifted compared with the expected value. This is most likely to be an artifact resulting from the P/4 leak subtraction combined with the small amount of extra sodium in the bath solution coming from the pH adjustment with NaOH, which may have slightly

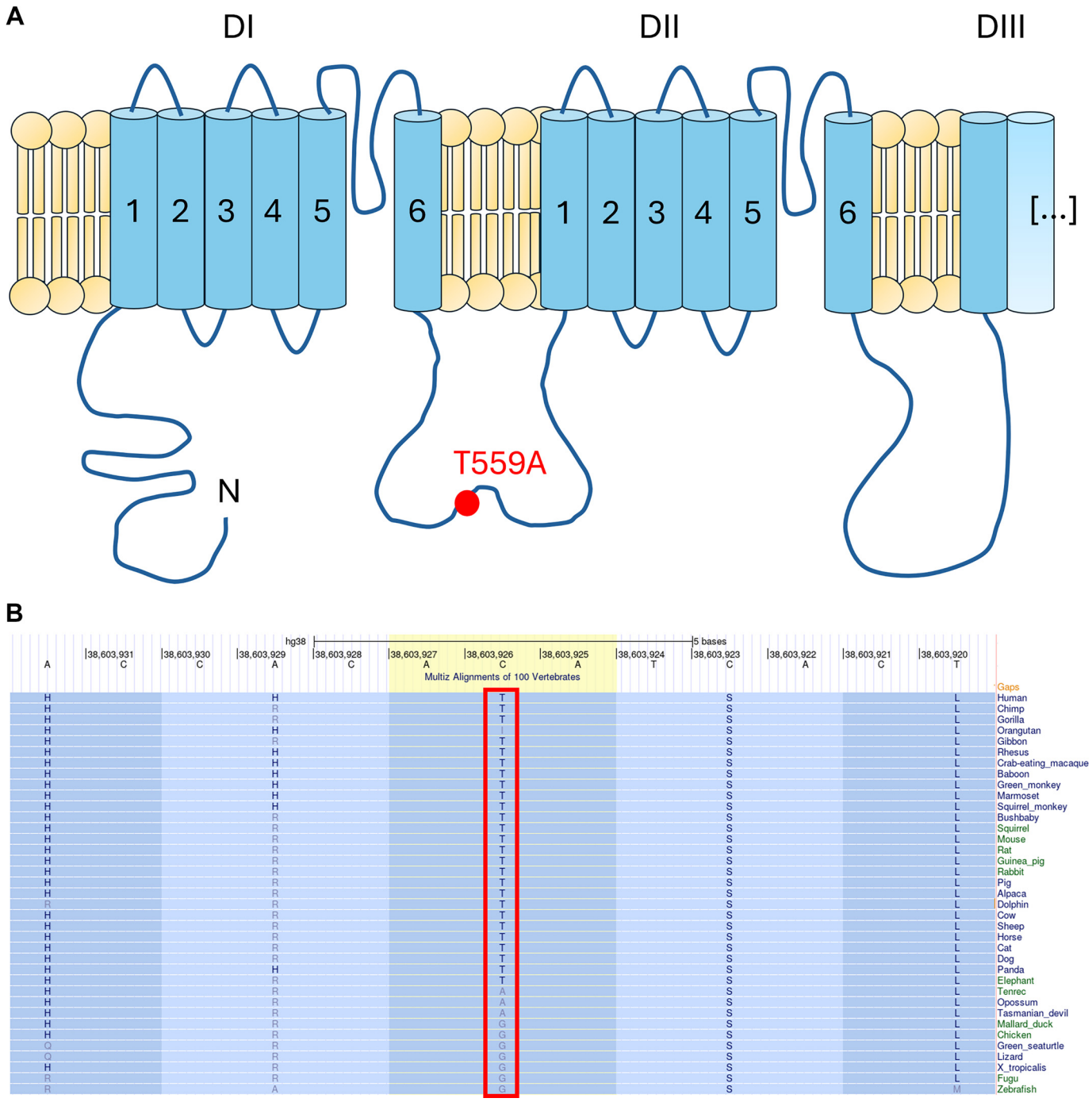


**Figure 1.** Location of T559A in the Nav1.5 protein. *A*: position of the mutation within the protein structure. For clarity, only the DI and DII domains are fully shown. *B*: multiple alignments of the region around T559 residue in different vertebrates (made with the UCSC Genome Browser multiple alignment tool).

increased the final sodium concentration. To study the voltage dependence of channel inactivation, a two-step protocol was used. Briefly, from a holding level of −120 mV, the first pulse consisted of a 500-ms step to potentials ranging from −140 to +10 mV, followed by a second 50 ms pulse to −20 mV. Peak currents at the second pulse (Fig. 2*C*) were normalized to their maximal value, plotted against the first pulse voltage and fitted with a Boltzmann sigmoidal equation (Fig. 2*D*). The voltage dependence of channel inactivation was unaffected by the reversion, whereas the voltage dependence of channel activation calculated from the *I-V* curve was slightly but significantly left-shifted by 3 mV (Fig. 2*D*, Table 1). However, such a small change would hardly have any functional relevance, and it was most probably an artifact due to the large difference in current density. Finally, the recovery from inactivation was not affected by the reversion (Table 1). These results strongly suggest that T559A causes a loss-of-function effect on the channel current density.

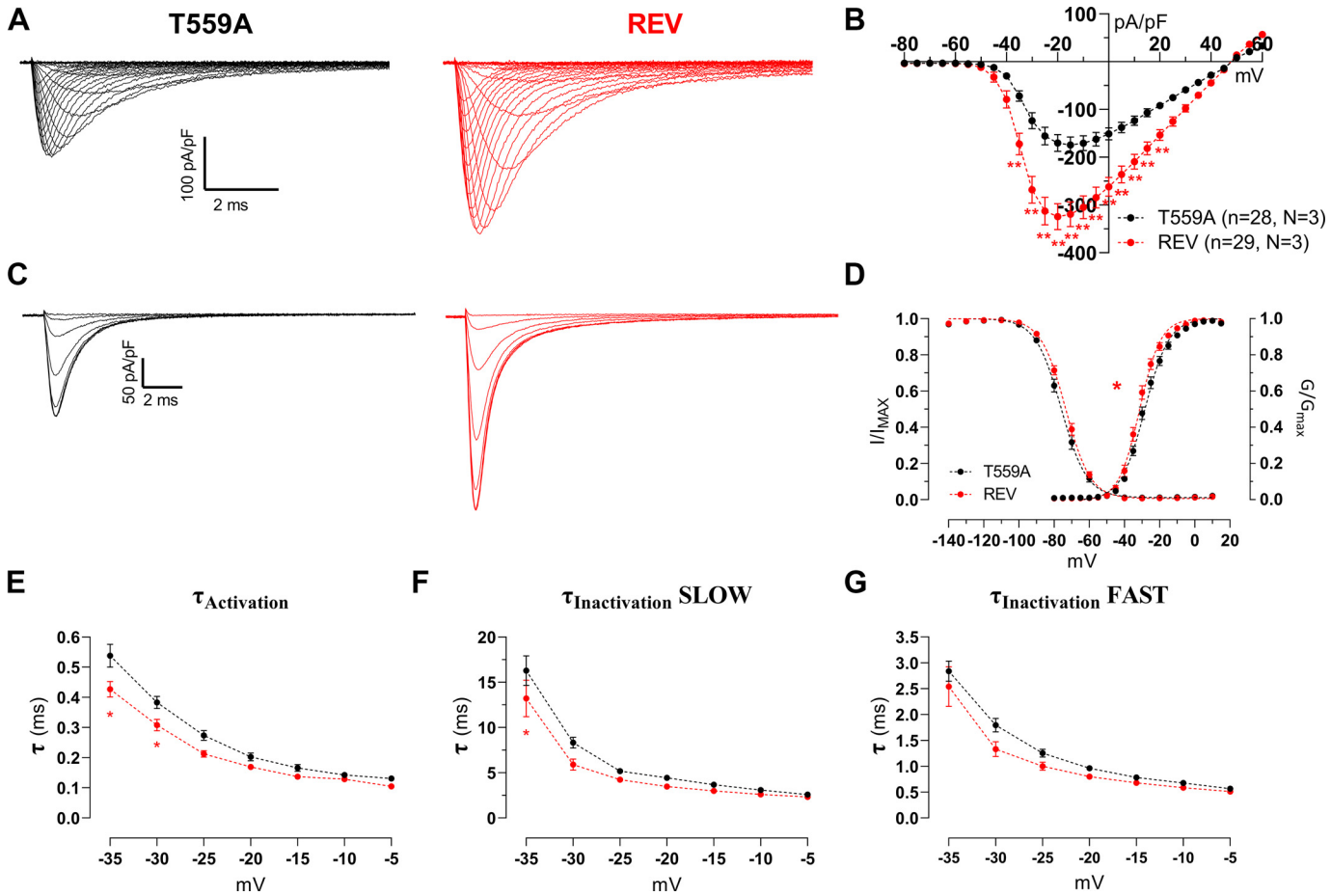


**Figure 2.** Effect of reverting T559A variant in Nav1.5 channel. *A*: representative traces of sodium currents of T559A and reverted (REV) channel elicited by 5 mV steps between −80 and +60 mV from a −120 mV holding potential. *B*: current-voltage relationship of T559A (black) and REV channel (red). *C*: sample traces of sodium currents of T559A and reverted channel elicited by a two pulses steady-state inactivation protocol. For the sake of clarity, only the second pulse of the voltage protocol is shown. *D*: voltage dependence of channel activation and inactivation. Experimental data were fitted with a Boltzmann sigmoidal function. Kinetics of channel activation (*E*) and of channel inactivation (*F* and *G*). Currents activating and inactivating decay were fitted with a single and biexponential function, respectively. (*$P < 0.05$ and **$P < 0.001$, two-way ANOVA with Sidak post hoc for multiple comparisons).

## The Reverted Channel has Faster Activation and Inactivation Kinetics

The time courses of channel activation and inactivation were analyzed by fitting the activating and inactivating current decays with a mono- or bi-exponential function, respectively. The reverted channel showed just slightly, yet significantly faster time constant for channel activation (Fig. 2*E*, Table 1) and the slow component of inactivation (Fig. 2*F*, Table 1), whereas the fast component of channel inactivation was slightly, but not significantly, accelerated by the reversion (Fig. 2*G*, Table 1).

**Table 1.** *Electrophysiological parameters of NaV1.5 T559A and reverted channel*

| Parameter | T559A | REV |
|---|---|---|
| Peak current density, pA/pF | −170.1 ± 17.7 ($n = 28$; $N = 3$) | −324.2 ± 27.4 ($n = 29$; $N = 3$)* |
| Maximal conductance (Gmax), nS | 45.2 ± 4.7 | 75.5 ± 7.1* |
| $V_{1/2}$ of activation, mV | −28.1 ± 0.8 | −31.2 ± 1.0* |
| Slope factor of activation, mV | 6.2 ± 0.3 | 5.0 ± 0.3 |
| $V_{1/2}$ of inactivation, mV | −75.7 ± 1.2 | −73.4 ± 0.9 |
| Slope factor of inactivation, mV | −6.2 ± 0.2 | −6.3 ± 0.1 |
| Activation τ at −35 mV, ms | 0.54 ± 0.04 | 0.43 ± 0.03* |
| Inactivation τ slow at −35 mV, ms | 16.3 ± 1.6 | 13.2 ± 2.0* |
| Inactivation τ fast at −35 mV, ms | 2.8 ± 0.2 | 2.5 ± 0.4 |
| Recovery from inactivation τ slow, ms | 120.6 ± 26.5 ($n = 24$; $N = 3$) | 140.2 ± 33.3 ($n = 25$; $N = 3$) |
| Recovery from inactivation τ fast, ms | 9.4 ± 0.6 | 8.6 ± 0.5 |
| Late current ($I_{Late}/I_{Peak}$) (% of the peak) | 0.27 ± 0.05 ($n = 16$; $N = 3$) | 0.23 ± 0.05 ($n = 16$; $N = 3$) |

Data are represented as means ± SE. REV, reverted. *$P < 0.05$ unpaired *t* test.

### T559A does not Affect the Sodium Late Current

Given that phosphorylation of the DI-DII loop regulates the late sodium current (15), we investigated whether the T559A variant influences this property. To do so, we used pharmacological subtraction of the TTX-sensitive current, elicited by a 200-ms repetitive pulse to −10 mV in 140 mM NaCl, before and after applying 30 μM TTX (Fig. 3*A*). The mean amplitude of the steady-state current at the end of the depolarizing pulse was then divided by the peak amplitude at the beginning of the pulse. The late current amplitude was then expressed as a percentage of the peak (Fig. 3*B*, Table 1). No significant difference was observed between the two channels.

## DISCUSSION

The hH1a *SCN5A* clone, which carries the T559A variant, has long been used as a wild-type control in electrophysiological studies. In this study, we present a functional characterization of the T559A variant. The reported data showed that the substitution of a threonine with an alanine led to a significant reduction in the current density, implying that the variant is not actually representative of the true wild-type sequence, as it introduces functional differences that may be interpreted as a loss-of-function of the cardiac sodium channel. Despite being a highly conserved residue in the Mammalia class (with the exception of the Orangutan), the pathophysiological relevance of T559 has never been fully clarified. Intriguingly, two distantly related marsupials and a Madagascar-native Tenrecidae carry an alanine in position 559, but the lack of functional information on these specific channels prevents the advancement of a solid hypothesis about the possible effects related to this alanine residue. T559 is located in the DI-DII intracellular loop of the Nav1.5 channel, which is a fundamental regulatory domain. In fact, it contains multiple phosphorylation sites that directly interact with the CaMKII kinases, the protein kinases A (PKA), and the serum- and glucocorticoid-inducible kinases (SGK) for the regulation of channel trafficking, kinetics, and voltage dependence (16). T559 itself has not been identified as a direct phosphorylation site, but with the subsequent serine in position 560 is part of the phosphopeptide 559-T(pS)LLVPWPLR (17). Together with the common polymorphism H558R and the L561 residue, T559 may indeed form a consensus sequence for the Akt/PKB kinases on S560 (18). Other close-by phosphorylation sites include S516, S525, S539, S549, S571, S581, and S593 (17). Moreover, it has been reported that mutations in threonine residues in the immediate surroundings can affect channel regulation by kinases. For example, the substitution of threonine in position 594 (T594A) inhibited the negative shift of channel availability upon CaMKII activation (14). A similar effect was observed for S571 (19). Despite the absence of fully compelling evidence, a potential role of T559 in the phosphoregulation of Nav1.5 cannot be excluded.

Overall, mutations in this region have been linked with different cardiac diseases, including Long QT syndrome, Brugada syndrome, cardiac conduction disease, sick sinus syndrome, and dilated cardiomyopathy (20–22). Two proarrhythmic variants (A572D and Q573E) are located in the immediate vicinity of S571 (16). According to the ClinVAr Miner database, the missense variant T559I that introduces the same residue found in Orangutans [NM_000335.5(SCN5A):c.1676C>T (p.Thr559Ile)] has been found in human individual(s) with dilated cardiomyopathy (23) and in heterozygosis in healthy controls (24). Because the available evidence is insufficient and no functional characterization has been performed, T559I is classified as a variant of unknown significance (VUS). Similarly, the T559K [NM_000335.5(SCN5A):c.1676C>A (p.Thr559Lys)] variant is also reported as a VUS (25). From the epidemiologic perspective, T559A is not a common polymorphism and is considered a rare variant of the channel that has never been associated with clinical reports. It is plausible to speculate that the T559A variant originated from the frozen biopsy tissue of diseased adult ventricular myocardium used in the original cloning of hH1a (2); however, definitive evidence to confirm this hypothesis is currently lacking. Because the hH1a clone is functional to an acceptable level, and in the absence of clinical evidence, the potential impact of T559A has been overlooked over the years. When acknowledged, the presence of this rare variant in WT control clones has been commented with "no functional consequences have been reported" (11) or "the effects of [. . .] T559A

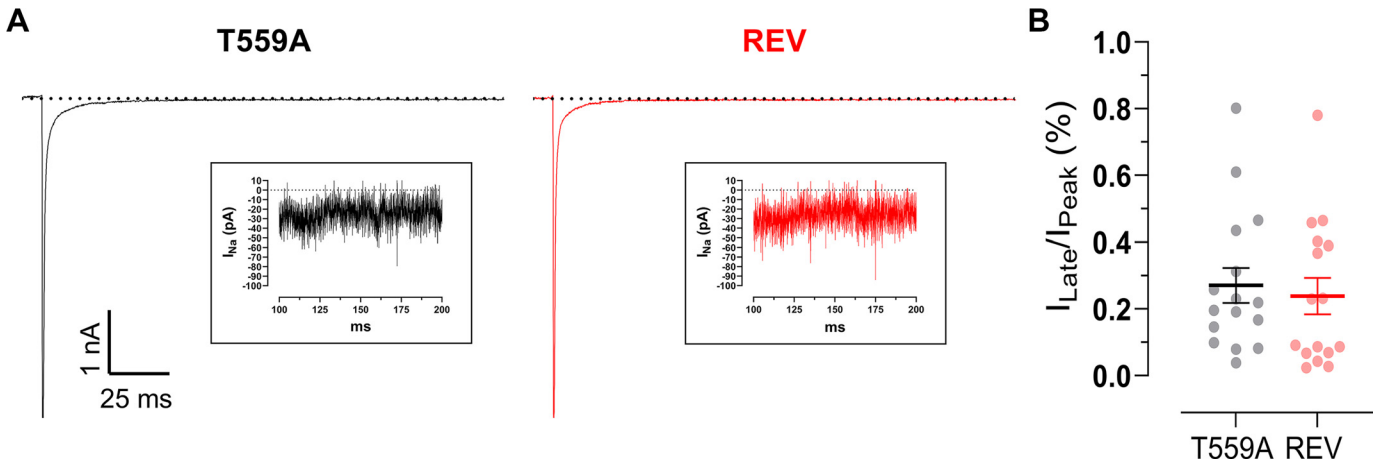


**Figure 3.** Effect of reverting T559A variant on the late sodium current. *A*: sample traces of tetrodotoxin (TTX) sensitive sodium currents of T559A and reverted (REV) channel elicited by a 200 ms depolarization step to −10 mV, with zoomed highlights of the pulse end in the onsets. *B*: late sodium current calculated as a percentage of the mean steady-state end-pulse current ($I_{Late}$) over the peak ($I_{Peak}$) of the TTX-sensitive current.

are unknown" (26). However, it is known that different genetic background can affect/mask the functional effects of other mutations through phenomenon such as "intragenic complementation." Indeed, the hH1b *SCN5A* clone that holds a threonine in position 559 and differs from both hH1 and hH1a for at least three residues, rescued the expression defect of LQT3 mutation M1766L when compared with the other two clones (4). In addition, the LQT3-related A572D mutation becomes proarrhythmic only in the presence of the common polymorphism H558R that is found in the hH1b clone (27). On the other hand, the trafficking defective Brugada syndrome-related R282H variant and the sick sinus syndrome-related variant D1275N are rescued by the presence of H558R (28, 29), suggesting a more complex interaction between pathogenic variants and common polymorphisms. In this context, it would be interesting in future to investigate the potential effect of T559A on the modulatory effect of H558R. In conclusion, by documenting the discrepancy between commonly used constructs and the actual human reference sequence, this work may serve as a cautionary example of how unnoticed sequence differences can introduce systematic bias into otherwise carefully designed studies. We hope that this report will help other laboratories to make informed decisions about which constructs to use or avoid as the most appropriate control for the functional characterization of pathological mutations to prevent the propagation of erroneous assumptions across multiple studies.

Good practice should include routinely sequencing of the available constructs, not overlooking the presence of rare variants, and critical re-evaluation of past results that used hH1a as a control. This has broad implications for reproducibility, particularly in studies using heterologous expression systems for channelopathy modeling.

## DATA AVAILABILITY

Data will be made available upon reasonable request.

## GRANTS

This project is supported by grant from Ministero dell'Universitàe della Ricerca-NextGenerationEU under Grant No. PNRR M4.C2.I1.1-Avviso 104/2022, CUP H53D23006370006 Project title "A study investigating post-translational modifications in Brugada Syndrome and their effects on cardiac activity using hIPSC-derived cardiomyocytes," and from the Ricerca Corrente funding provided by the Italian Ministry of Health to IRCCS Policlinico San Donato and by IRCCS Policlinico San Donato own funds.

## DISCLOSURES

No conflicts of interest, financial or otherwise, are declared by the authors.

## AUTHOR CONTRIBUTIONS

D.M., M.V., L.A., and I.R. conceived and designed research; D.M., M.V., A.F., and S.C. performed experiments; D.M. and M.V. analyzed data; D.M., M.V., L.A., and I.R. interpreted results of experiments; D.M. prepared figures; D.M. drafted manuscript; D.M., M.V., A.F., S.C., L.A., C.P., and I.R. edited and revised manuscript; L.A., C.P., and I.R. approved final version of manuscript.

## REFERENCES

1. **Gellens ME**, **George AL Jr**, **Chen LQ**, **Chahine M**, **Horn R**, **Barchi RL**, **Kallen RG.** Primary structure and functional expression of the human cardiac tetrodotoxin-insensitive voltage-dependent sodium channel. *Proc Natl Acad Sci USA* 89: 554–558, 1992. doi:10.1073/pnas.89.2.554.
2. **Hartmann HA**, **Tiedeman AA**, **Chen SF**, **Brown AM**, **Kirsch GE.** Effects of III-IV linker mutations on human heart $Na^+$ channel inactivation gating. *Circ Res* 75: 114–122, 1994. doi:10.1161/01.res.75.1.114.
3. **Makielski JC**, **Ye B**, **Valdivia CR**, **Pagel MD**, **Pu J**, **Tester DJ**, **Ackerman MJ.** A ubiquitous splice variant and a common polymorphism affect heterologous expression of recombinant human SCN5A heart sodium channels. *Circ Res* 93: 821–828, 2003. doi:10.1161/01.RES.0000096652.14509.96.
4. **Ye B**, **Valdivia CR**, **Ackerman MJ**, **Makielski JC.** A common human SCN5A polymorphism modifies expression of an arrhythmia causing mutation. *Physiol Genomics* 12: 187–193, 2003. doi:10.1152/physiolgenomics.00117.2002.
5. **Rougier JS**, **van Bemmelen MX**, **Bruce MC**, **Jespersen T**, **Gavillet B**, **Apothéloz F**, **Cordonier S**, **Staub O**, **Rotin D**, **Abriel H.** Molecular determinants of voltage-gated sodium channel regulation by the Nedd4/Nedd4-like proteins. *Am J Physiol Cell Physiol* 288: C692–C701, 2005. doi:10.1152/ajpcell.00460.2004.
6. **Keller DI**, **Rougier JS**, **Kucera JP**, **Benammar N**, **Fressart V**, **Guicheney P**, **Madle A**, **Fromer M**, **Schläpfer J**, **Abriel H.** Brugada syndrome and fever: genetic and molecular characterization of patients carrying SCN5A mutations. *Cardiovasc Res* 67: 510–519, 2005. doi:10.1016/j.cardiores.2005.03.024.
7. **Cordeiro JM**, **Barajas-Martinez H**, **Hong K**, **Burashnikov E**, **Pfeiffer R**, **Orsino AM**, **Wu YS**, **Hu D**, **Brugada J**, **Brugada P**, **Antzelevitch C**, **Dumaine R**, **Brugada R.** Compound heterozygous mutations P336L and I1660V in the human cardiac sodium channel associated with the Brugada syndrome. *Circulation* 114: 2026–2033, 2006. doi:10.1161/CIRCULATIONAHA.106.627489.
8. **Hu D**, **Viskin S**, **Oliva A**, **Carrier T**, **Cordeiro JM**, **Barajas-Martinez H**, **Wu Y**, **Burashnikov E**, **Sicouri S**, **Brugada R**, **Rosso R**, **Guerchicoff A**, **Pollevick GD**, **Antzelevitch C.** Novel mutation in the SCN5A gene associated with arrhythmic storm development during acute myocardial infarction. *Heart Rhythm* 4: 1072–1080, 2007. doi:10.1016/j.hrthm.2007.03.040.
9. **Pfahnl AE**, **Viswanathan PC**, **Weiss R**, **Shang LL**, **Sanyal S**, **Shusterman V**, **Kornblit C**, **London B**, **Dudley SC Jr.** A sodium channel pore mutation causing Brugada syndrome. *Heart Rhythm* 4: 46–53, 2007. doi:10.1016/j.hrthm.2006.09.031.
10. **Clatot J**, **Ziyadeh-Isleem A**, **Maugenre S**, **Denjoy I**, **Liu H**, **Dilanian G**, **Hatem SN**, **Deschênes I**, **Coulombe A**, **Guicheney P**, **Neyroud N.** Dominant-negative effect of SCN5A N-terminal mutations through the interaction of Na(v)1.5 $\alpha$-subunits. *Cardiovasc Res* 96: 53–63, 2012. doi:10.1093/cvr/cvs211.
11. **Wang Z**, **Vermij SH**, **Sottas V**, **Shestak A**, **Ross-Kaschitza D**, **Zaklyazminskaya EV**, **Hudmon A**, **Pitt GS**, **Rougier JS**, **Abriel H.** Calmodulin binds to the N-terminal domain of the cardiac sodium channel Nav1.5. *Channels (Austin)* 14: 268–286, 2020. doi:10.1080/19336950.2020.1805999.
12. **Dahlberg P**, **Pozzi S**, **Bulmer L**, **Golluscio A**, **Nilsson M**, **Nygren A**, **Larsson HP**, **Pantazis A**, **Gummesson A.** Clinical and electrophysiological characterization of a SCN5A gain-of-function mutation associated with CPVT-like arrhythmia. *J Mol Cell Cardiol* 203: 47–58, 2025. doi:10.1016/j.yjmcc.2025.04.001.
13. **Frosio A**, **Micaglio E**, **Polsinelli I**, **Calamaio S**, **Melgari D**, **Prevostini R**, **Ghiroldi A**, **Binda A**, **Carrera P**, **Villa M**, **Mastrocinque F**, **Presi S**, **Salerno R**, **Boccellino A**, **Anastasia L**, **Ciconte G**, **Ricagno S**, **Pappone C**, **Rivolta I.** Unravelling Novel SCN5A mutations linked to Brugada syndrome: functional, structural, and genetic insights. *Int J Mol Sci* 24: 15089, 2023. doi:10.3390/ijms242015089.
14. **Ashpole NM**, **Herren AW**, **Ginsburg KS**, **Brogan JD**, **Johnson DE**, **Cummins TR**, **Bers DM**, **Hudmon A.** $Ca^{2+}$/calmodulin-dependent protein kinase II (CaMKII) regulates cardiac sodium channel NaV1.5 gating by multiple phosphorylation sites. *J Biol Chem* 287: 19856–19869, 2012. doi:10.1074/jbc.M111.322537.
15. **Glynn P**, **Musa H**, **Wu X**, **Unudurthi SD**, **Little S**, **Qian L**, **Wright PJ**, **Radwanski PB**, **Gyorke S**, **Mohler PJ**, **Hund TJ.** Voltage-gated sodium channel phosphorylation at Ser571 regulates late current,

arrhythmia, and cardiac function in vivo. *Circulation* 132: 567–577, 2015. doi:10.1161/CIRCULATIONAHA.114.015218.

16. **Marionneau C**, **Abriel H.** Regulation of the cardiac $Na^+$ channel NaV1.5 by post-translational modifications. *J Mol Cell Cardiol* 82: 36–47, 2015. doi:10.1016/j.yjmcc.2015.02.013.
17. **Lorenzini M**, **Burel S**, **Lesage A**, **Wagner E**, **Charrière C**, **Chevillard PM**, **Evrard B**, **Maloney D**, **Ruff KM**, **Pappu RV**, **Wagner S**, **Nerbonne JM**, **Silva JR**, **Townsend RR**, **Maier LS**, **Marionneau C.** Proteomic and functional mapping of cardiac NaV1.5 channel phosphorylation sites. *J Gen Physiol* 153: e202012646, 2021. doi:10.1085/jgp.202012646.
18. **Rust HL**, **Thompson PR.** Kinase consensus sequences: a breeding ground for crosstalk. *ACS Chem Biol* 6: 881–892, 2011. doi:10.1021/cb200171d.
19. **Hund TJ**, **Koval OM**, **Li J**, **Wright PJ**, **Qian L**, **Snyder JS**, **Gudmundsson H**, **Kline CF**, **Davidson NP**, **Cardona N**, **Rasband MN**, **Anderson ME**, **Mohler PJ.** A β(IV)-spectrin/CaMKII signaling complex is essential for membrane excitability in mice. *J Clin Invest* 120: 3508–3519, 2010. doi:10.1172/JCI43621.
20. **Zimmer T**, **Surber R.** SCN5A channelopathies—an update on mutations and mechanisms. *Prog Biophys Mol Biol* 98: 120–136, 2008. doi:10.1016/j.pbiomolbio.2008.10.005.
21. **Ruan Y**, **Liu N**, **Priori SG.** Sodium channel mutations and arrhythmias. *Nat Rev Cardiol* 6: 337–348, 2009. doi:10.1038/nrcardio.2009.44.
22. **Kapplinger JD**, **Tester DJ**, **Alders M**, **Benito B**, **Berthet M**, **Brugada J**, **Brugada P**, **Fressart V**, **Guerchicoff A**, **Harris-Kerr C**, **Kamakura S**, **Kyndt F**, **Koopmann TT**, **Miyamoto Y**, **Pfeiffer R**, **Pollevick GD**, **Probst V**, **Zumhagen S**, **Vatta M**, **Towbin JA**, **Shimizu W**, **Schulze-Bahr E**, **Antzelevitch C**, **Salisbury BA**, **Guicheney P**, **Wilde AA**, **Brugada R**, **Schott JJ**, **Ackerman MJ.** An international compendium of mutations in the SCN5A-encoded cardiac sodium channel in patients referred for Brugada syndrome genetic testing. *Heart Rhythm* 7: 33–46, 2010. doi:10.1016/j.hrthm.2009.09.069.
23. **Mazzarotto F**, **Tayal U**, **Buchan RJ**, **Midwinter W**, **Wilk A**, **Whiffin N**, **Govind R**, **Mazaika E**, **de Marvao A**, **Dawes TJW**, **Felkin LE**, **Ahmad M**, **Theotokis PI**, **Edwards E**, **Ing AY**, **Thomson KL**, **Chan LLH**, **Sim D**, **Baksi AJ**, **Pantazis A**, **Roberts AM**, **Watkins H**, **Funke B**, **O'Regan DP**, **Olivotto I**, **Barton PJR**, **Prasad SK**, **Cook SA**, **Ware JS**, **Walsh R.** Reevaluating the genetic contribution of monogenic dilated cardiomyopathy. *Circulation* 141: 387–398, 2020. doi:10.1161/CIRCULATIONAHA.119.037661.
24. **Fang DH**, **Wu LQ**, **Lu L**, **Lou S**, **Gu G**, **Chen QJ**, **Pu LJ**, **Shen WF.** Association of human SCN5A polymorphisms with idiopathic ventricular arrhythmia in a Chinese Han cohort. *Circ J* 72: 592–597, 2008. doi:10.1253/circj.72.592.
25. **Nykamp K**, **Anderson M**, **Powers M**, **Garcia J**, **Herrera B**, **Ho YY**, **Kobayashi Y**, **Patil N**, **Thusberg J**, **Westbrook M**, **Topper S**; **Invitae Clinical Genomics Group.** Sherloc: a comprehensive refinement of the ACMG-AMP variant classification criteria. *Genet Med* 19: 1105–1117, 2017 [Erratum in *Genet Med* 22: 240, 2020]. doi:10.1038/gim.2017.37.
26. **Tan BH**, **Valdivia CR**, **Song C**, **Makielski JC.** Partial expression defect for the SCN5A missense mutation G1406R depends on splice variant background Q1077 and rescue by mexiletine. *Am J Physiol Heart Circ Physiol* 291: H1822–H1828, 2006. doi:10.1152/ajpheart.00101.2006.
27. **Tester DJ**, **Valdivia C**, **Harris-Kerr C**, **Alders M**, **Salisbury BA**, **Wilde AA**, **Makielski JC**, **Ackerman MJ.** Epidemiologic, molecular, and functional evidence suggest A572D-SCN5A should not be considered an independent LQT3-susceptibility mutation. *Heart Rhythm* 7: 912–919, 2010. doi:10.1016/j.hrthm.2010.04.014.
28. **Poelzing S**, **Forleo C**, **Samodell M**, **Dudash L**, **Sorrentino S**, **Anaclerio M**, **Troccoli R**, **Iacoviello M**, **Romito R**, **Guida P**, **Chahine M**, **Pitzalis M**, **Deschênes I.** SCN5A polymorphism restores trafficking of a Brugada syndrome mutation on a separate gene. *Circulation* 114: 368–376, 2006. doi:10.1161/CIRCULATIONAHA.105.601294.
29. **Gui J**, **Wang T**, **Trump D**, **Zimmer T**, **Lei M.** Mutation-specific effects of polymorphism H558R in SCN5A-related sick sinus syndrome. *J Cardiovasc Electrophysiol* 21: 564–573, 2010. doi:10.1111/j.1540-8167.2010.01762.x.